Oscillation of dynamic conductance of Al-C_n-Al structures: Nonequilibrium Green's function and density functional theory study

Bin Wang,[1] Yunjin Yu,[2] Lei Zhang,[1] Yadong Wei,[2] and Jian Wang[1,*]

[1]*Department of Physics and The Center of Theoretical and Computational Physics, The University of Hong Kong, Pokfulam Road, Hong Kong, China*

[2]*School of Physics, Shenzhen University, Shenzhen, 518060 China*

(Received 8 January 2009; published 22 April 2009)

Using the nonequilibrium Green's function combined with the density functional theory, we investigate the dynamic conductance of atomic wires consisting 4–9 carbon atoms in contact with two Al(100) electrodes. Our numerical results show that in addition to the dc conductance, both the real part and imaginary part of dynamic conductance show oscillatory behaviors for even-odd number of carbon atoms at low frequencies. Interestingly, the dynamic part of the ac conductance depends only on the parity of the number of carbon atoms n, i.e., whether n is even or odd. These oscillations of dynamic conduction can be understood by analyzing the average transmission coefficient T_{av} and the global density of states.

DOI: 10.1103/PhysRevB.79.155117 PACS number(s): 85.35.−p, 85.65.+h

I. INTRODUCTION

As the ultimate limit of the miniaturization of electrical conductors, atomic-wire based tunneling junction has been considered as a basic building block of nanodevices. Apart from possible technological applications such as interconnects in molecular electronics,[1–3] atomic-wire structures are also interesting from the scientific point of view since much physical insight can be obtained in understanding electron transport in nanometer scales.[4–8] For instance, using the Lippmann-Schwinger equation coupled with density functional theory (DFT), Lang[4] calculated the conductance of atomic carbon wires and predicted negative differential resistance in the tunneling regime. By combining DFT with the solution of three-dimensional quantum-scattering problem, quantized conductance was observed for Al and Si wires consisting of two or more atoms.[5,6]

One of the interesting features of transport in atomic-wire structures is the oscillatory behaviors of transport properties, such as dc conductance,[9–13] thermopower and thermoconductance,[14] against the even-odd number of atoms in the scattering region. For instance, Lang *et al.*[13] predicted the conductance oscillation against the even-odd carbon atoms and explained the physical origin by analyzing the occupation states of π electrons in the conduction bands and valance bands.[13] Due to the charge transfer, it was found that thermopower and thermoconductance of Al-C_n-Al structures also exhibit oscillatory behaviors[14] against the even-odd number of carbon atoms. Using STM and the mechanically controlled break junctions, the even-odd oscillations of dc conductance for Au, Pt, and Ir have been confirmed experimentally suggesting it to be a universal feature of atomic wires.[15] So far all the investigations on atomic wires are limited to the dc conductance, less attention is focused on the ac conductance.[16] It would be interesting to know whether the dynamic conductance has similar oscillatory behavior as that of dc conductance. In the presence of ac field, the system is out of equilibrium. Due to the charge accumulation in the scattering region, the particle current alone is not a conserved quantity. The displacement current due to the long-range Coulomb interaction has to be included.[17–19] In this paper we present the first-principles calculation of the dynamic conductance $G(\omega)$ of Al-C_n-Al structures. We found that in addition to the dc conductance G_{dc}, the real part and imaginary part of dynamic conductance, also show the even-odd oscillations against the number of carbon atoms. Remarkably, the dynamic part of ac conductance $G(\omega)$-G_{dc} depends only on the parity of the number of carbon atoms, i.e., whether n is even or odd, at low frequencies up to terahertz range. Intuitively, if a system is highly transmissive with a large transmission coefficient, it behaves like an inductor and the dynamic response is inductivelike. On the other hand if a system does not conduct well with small transmission coefficient, it behaves like a capacitor and shows a capacitivelike behavior under ac bias. For Al-C_n-Al structures, our results show that although the total transmission coefficients are larger than one, all the carbon chains exhibit capacitivelike behaviors. Our results indicate that it is the averaged transmission coefficient[20] T_{av} that determines the dynamic response of the system and T_{av}'s are much smaller than one.

II. THEORETICAL FORMALISM

Figure 1 depicts the schematic Al-C_n-Al structure that we considered in this paper. The system consists of a short carbon chain C_n that is in contact with electron reservoirs through two semi-infinite Al electrodes. The unit cell of the

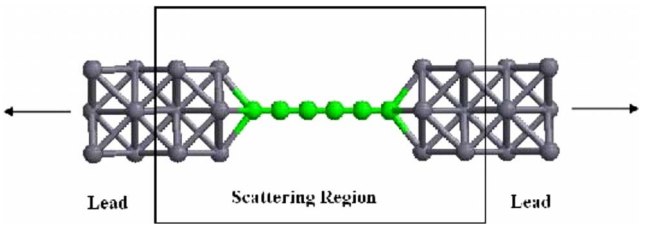

FIG. 1. (Color online) The schematic structure of Al-C_6-Al system. An atomic wire with six carbon atoms is sandwiched between two semi-infinite atomic Al electrodes. The Al electrodes extend to $\pm\infty$ along (100) direction where the electric current is collected. The center box denotes the simulation region in the NEGF+DFT method.

semi-infinite Al electrodes contains 18 atoms with a cross section along (100) direction. In our calculation, we have varied the number of carbon atoms from four to nine while fixing the configuration of Al atomic electrodes. The distance between the neighboring carbon atoms is equal to 2.5 a.u and between the end carbon atom and the Al electrode is equal to 3.78 a.u. These distances as well as the entire device structure are determined in dc condition and may be relaxed further under ac condition. This should in principle be determined under the ac transport condition self-consistently. However, how to calculate quantum-mechanical forces under an ac current flow is still an unsolved problem.[21] Since we are interested in the dynamic conductance at small bias, the effect of current on atomic structure is small. We therefore neglect this piece of physics as an approximation for our model analysis and use similar data used in Ref. 9. However, the Coulomb interaction induced by ac current will be included implicitly (see discussion below).

In order to calculate the dynamic conductance of atomic carbon chains, we use state-of-the-art first-principles quantum transport package MATDCAL[22,23] where DFT is carried out within the formalism of the Keldysh nonequilibrium Green's function (NEGF). In our calculation, a linear combination of the atomic orbitals (LCAO) basis set[24] is employed to solve the Kohn-Sham (KS) equations numerically. The exchange-correlation is treated at the LDA level and a nonlocal norm conserving pseudopotential[25] is used to define the atomic core. The atomic structure and system Hamiltonian are determined by DFT, and the nonequilibrium transport properties are determined by NEGF. Real space numerical techniques are used to deal with the transport boundary conditions under external bias. The basic principle and practical implementation of the NEGF-DFT formalism can be found in Ref. 26. In our calculation, the NEGF-DFT self-consistency was carried out until the numerical tolerance is less than 10^{-4}.

The dynamic conductance of the system is evaluated using the following expression, which is derived using NEGF:[19]

$$G_{\alpha\beta}(\omega) = G^c_{\alpha\beta}(\omega) - G^d_{\beta}(\omega)\frac{\sum_\gamma G^c_{\alpha\gamma}(\omega)}{\sum_\gamma G^d_{\gamma}(\omega)}, \tag{1}$$

where the subscripts α, β and $\gamma=L$ or R label Al electrodes. Here $G^c_{\alpha\beta}$ is the dynamic conductance due to the particle current and G^d_β is the contribution from the displacement current, which are all frequency dependent. Equation (1) is a general expression of dynamic response which is suitable for a variety of systems near or far from equilibrium. In the wideband limit where the self-energy is not very sensitive to the energy, the particle conductance $G^c_{\alpha\beta}(\omega)$ can be expressed as ($\hbar=1$),[19]

$$G^c_{\alpha\beta}(\omega) = -\int \frac{dE}{2\pi}\frac{f-\bar{f}}{\omega}\mathrm{Tr}[-\bar{G}^r_0\Gamma_\beta G^a_0\Gamma_\alpha + \bar{G}^r_0\Gamma G^a_0\Gamma_\alpha\delta_{\alpha\beta} - i\omega\bar{G}^r_0 G^a_0\Gamma_\alpha\delta_{\alpha\beta}], \tag{2}$$

where G^r_0 is the equilibrium Green's function and $\bar{G}^r_0 = G^r_0(E+\omega)$; Γ_α is the linewidth function which describes the coupling strength between the α lead and the scattering region and is related to the imaginary part of the self-energy function of semi-infinite electrode; f and $\bar{f}=f(E+\omega)$ are the Fermi distribution functions; The displacement current G^d_β is defined as[19]

$$G^d_\beta = -q\omega\int \frac{dE}{2\pi}\mathrm{Tr}[\bar{g}^<_\beta], \tag{3}$$

where $-iq\bar{g}^<_\beta = q\bar{G}^r_0\Gamma_\beta G^a_0(f-\bar{f})/\omega$ is the nonequilibrium charge distribution in the scattering region due to the ac field. This term is essential to ensure the current conservation and gauge invariance, i.e., $\Sigma_\alpha G_{\alpha\beta}=0$ (current conserving) and $\Sigma_\beta G_{\alpha\beta}=0$ (gauge invariance).

To see why the second term in Eq. (1) corresponds to the contribution from Coulomb interaction, we define the particle current $I^c_\alpha(\omega)=\Sigma_\beta G^c_{\alpha\beta}(\omega)v_\beta$. It is easy to show that

$$\sum_\alpha I^c_\alpha(\omega) = i\omega Q(\omega), \tag{4}$$

where $i\omega Q(\omega)=\Sigma_\beta G^d_\beta$ corresponds to the ac charge accumulation in the scattering region. This charge is related to the displacement field $\mathbf{D}$ of the internal Coulomb potential via Poisson equation,[18]

$$\nabla\cdot\mathbf{D}(\mathbf{r},\omega) = 4\pi\rho(\mathbf{r},\omega)$$

or

$$\Phi_E(\omega) = 4\pi Q(\omega),$$

where $\Phi_E(\omega)=\int d\mathbf{s}\cdot\mathbf{D}(\mathbf{r},\omega)$ is the electric flux and $Q=\int\rho(\mathbf{r})d\mathbf{r}$ is the total charge accumulation inside the scattering region. According to the classical physics the displacement current is defined as

$$I^d(t) = \frac{1}{4\pi}\frac{d\Phi_E(t)}{dt}$$

or

$$I^d(\omega) = -\frac{i\omega}{4\pi}\Phi_E(\omega) = -i\omega Q(\omega)$$

in Fourier space. Hence the time derivative of the pile-up charge is the total displacement current: $\Sigma_\alpha I^d_\alpha = dQ/dt$. Equation (1) has partitioned the total displacement current into each lead using the requirement of current conserving and gauge-invariant condition.[17,19]

In the low-frequency limit, the dynamic conductance in Eq. (1) can be expanded in terms of frequency ω as following:[27]

$$G_{\alpha\beta}(\omega) = G_{0,\alpha\beta} - i\omega E_{\alpha\beta} + \omega^2 K_{\alpha\beta} + O(\omega^3), \tag{5}$$

where $G_{0,\alpha\beta}$ is the dc conductance; $E_{\alpha\beta}$ is called emittance and characterizes the phase difference between the current

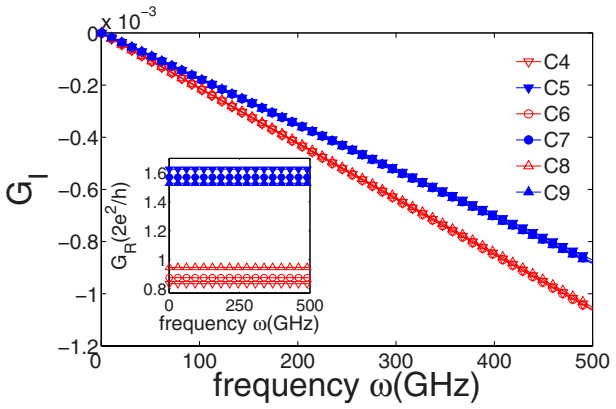

FIG. 2. (Color online) Imaginary part of dynamic conductance G_I versus frequency for Al-C_n-Al structure, here $n=4,5,6,7,8,9$. Inset: real part of dynamic conductance G_R versus frequency. Here C_4, C_5, C_6, C_7, C_8, and C_9 are described by open down triangle, solid down triangle, open circle, solid circle, open up triangle, and solid up triangle, respectively.

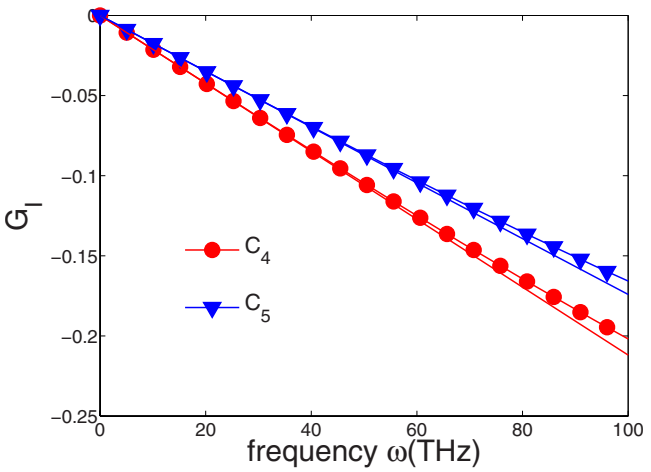

FIG. 3. (Color online) G_I versus frequency for Al-C_n-Al structures ($n=4$ solid circle and $n=5$ solid triangle). ωE_{12} is labeled by the straight lines.

and voltage at low frequency; $K_{\alpha\beta}$ describes the low-frequency dynamic dissipation. In terms of partial density of states (DOS),[18] emittance is defined as

$$E_{\alpha\beta} = \mathrm{Tr}\left[\frac{dn_{\alpha\beta}}{dE}\right] - \frac{\mathrm{Tr}[dn_\alpha/dE]\mathrm{Tr}[dn_\beta/dE]}{\mathrm{Tr}[dn/dE]}, \tag{6}$$

where $dn_{\alpha\beta}/dE$ is the partial density of states defined as[28]

$$\frac{dn_{\alpha\beta}}{dE} = \frac{1}{2\pi}\mathrm{Re}(\delta_{\alpha\beta}[G^r\Gamma_\alpha G^r] + i[G^r\Gamma_\beta G^a\Gamma_\alpha G^r]). \tag{7}$$

Here $dn_\alpha/dE=\Sigma_\beta dn_{\alpha\beta}/dE$ is the injectivity describing the local DOS when an incoming electron is injected from the α electrode and $dn/dE=\Sigma_\alpha dn_\alpha/dE$ is the total local DOS. In the case of single-channel transmission, the sign of $E_{\alpha\beta}$ determines the dynamic response of the system (either capacitivelike or inductivelike). For instance, if E_{11} is positive, the system shows capacitivelike behavior and while for the negative E_{11} the system behaves inductivelike.[18] For emittance, the current conserving and gauge-invariant conditions are also satisfied, i.e., $\Sigma_\alpha E_{\alpha\beta}=0$ and $\Sigma_\beta E_{\alpha\beta}=0$. Hence for a two-probe system, we have $E_{11}=-E_{12}$.

III. NUMERICAL RESULTS

Using Eq. (1), we calculated the dynamic conductance $G_{\alpha\beta}$ of Al-C_n-Al structures as a function of frequency. The inset of Fig. 2 shows the real part G_R of dynamic conductance with $G_R \equiv \mathrm{Re}(G_{11})$. At frequencies up to 500 GHz, dynamic conductance G_R is almost a constant equal to the dc conductance (we will get back to this later on). Note that G_R for atomic wires with even atoms (red curves) is smaller than that with odd atoms (blue curves) and therefore oscillates against the number n, which is consistent with the calculation of dc conductance.[9,13] The main panel of Fig. 2 shows the imaginary part G_I of dynamic conductance as a function of frequency for different number of carbon atoms n. For both even and odd carbon wires, G_I's are negative and decrease linearly in frequency with a larger decreasing rate for even number carbon wires than that of odd number carbon wires. Importantly, it shows that the imaginary part of dynamic conductance depends approximately only on the parity of n (the number of carbon atoms) and approximately obeys a linear relation up to 500 GHz,

$$G_I(\omega) = -a\omega, \tag{8}$$

where a is a constant and assumes only two values for even or odd number of carbon atoms.

At relatively low frequencies such as 500 GHz (corresponds to 13 meV), the imaginary part of the dynamical conductance is largely contributed by the emittance. The linear decrease in G_I from zero to a negative value corresponds to a positive E_{11} according to Eq. (5). To see the behavior of the imaginary part of dynamic conductance G_I at a larger frequency, we plot in Fig. 3 G_I versus frequency for different number of carbon atoms.[29] Since G_I of all even (or odd) number of carbon atoms collapses into one curve, we have shown G_I in Fig. 3 only for $n=4,5$. For comparison, we also depict emittance $E_{12}=-E_{11}$ calculated using Eq. (6). As expected, at small frequencies G_I is very close to ωE_{12} for both even and odd carbon atoms. While for a larger frequency, G_I is larger than ωE_{12} due to the contribution from $O(\omega^n)$ terms $(n \geq 2)$.

The oscillatory behaviors in Fig. 3 against the even-odd number of carbon atoms can be understood qualitatively as follows. Considering a symmetric system with only one transmission channel, the emittance is given by

$$E_{11} = \frac{dN_{11}}{dE} - \frac{1}{4}\frac{dN}{dE} = -\frac{1}{4}(2T-1)\frac{dN}{dE}, \tag{9}$$

where T is the transmission coefficient, $dN_\alpha/dE = \mathrm{Tr}[dn_\alpha/dE]$, and we have used the fact that $dN_1/dE = dN_2/dE$ for the symmetric system. Hence the sign of the

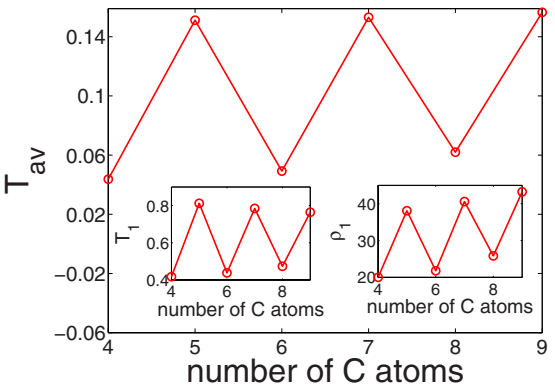

FIG. 4. (Color online) T_{av} versus the number of carbon atoms of Al-C_n-Al structure. Inset 1: T_1 versus the number of carbon atoms. Inset 2: ρ_1 versus the number of carbon atoms.

emittance is solely determined by the transmission coefficient T for a single transmission channel. While for a multichannel case, we have similar expression of the emittance except that T should be replaced with T_{av},

$$E_{11} = -\frac{1}{4}(2T_{\mathrm{av}} - 1)\frac{dN}{dE}, \tag{10}$$

where T_{av} is the average transmission coefficient defined as[20]

$$T_{\mathrm{av}} = \frac{\sum_n T_n \rho_n}{\mathrm{Tr}[dn/dE]}. \tag{11}$$

Here T_n is the nth eigenvalue of the transmission matrix $T = \Gamma_L G^r \Gamma_R G^a$ with the corresponding eigenfunction ϕ_n, and ρ_n is the effective projection of dn/dE onto ϕ_n.[30] From Eq. (10), we see that it is the averaged transmission coefficient T_{av} along with DOS determines the properties of emittance. If $T_{\mathrm{av}} > 1/2$, then $E_{11} < 0$ and the system shows inductivelike behavior and otherwise capacitivelike. Note that in general we have $T_{\mathrm{av}} \leq T$. Therefore, for a multichannel transmission, E_{11} can be positive even though T is larger than 1/2. For all Al-C_n-Al structures, there are seven transmission channels for incoming electron at Fermi level. Due to the quantum interference between the carbon chain and Al electrodes, there are only two degenerating channels (over 95%) dominate the transport at Fermi level. For example, when the number of carbon atoms $n=4$, the dominating transmission coefficients are $T_1 = T_2 = 0.396$, with $\rho_1 = \rho_2 = 40.3$; while for $n=5$, $T_1 = T_2 = 0.810$, and $\rho_1 = \rho_2 = 46.7$. Using Eq. (11), T_{av} is calculated and shown in Fig. 4 against the number of carbon atoms. Since the oscillation of T_{av} is determined by the oscillation of T_n and ρ_n, we have also plotted T_1 and ρ_1 vs the number of carbon atoms in the insets of Fig. 4. We found the averaged transmission coefficients T_{av} are much smaller than 1/2 for both even and odd number of carbon atoms although the total transmission coefficients T for all the carbon wires are larger than 1/2. Therefore, E_{11}'s are positive for all the carbon atomic-wire systems exhibiting capacitivelike behaviors. From insets of Fig. 3 we see that T_1 and ρ_1 oscillate with similar pattern as that of dc conductance of carbon chains. Since there are only two degenerate channels dominating the transport in carbon chains, we rewrite Eq. (10) as

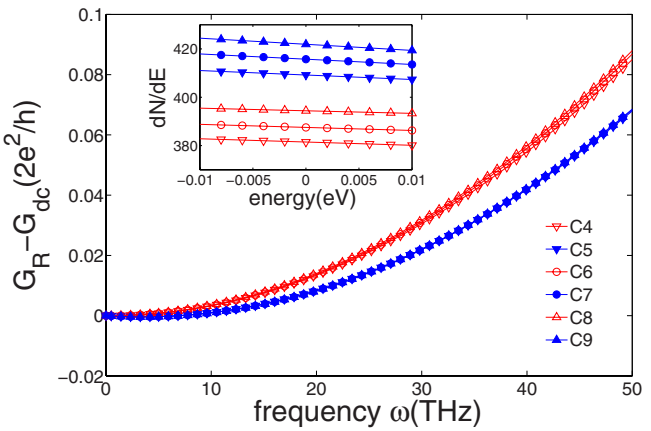

FIG. 5. (Color online) Real part of $G_{11}(\omega)$ subtracted by dc conductance, G_R-G_{dc}, versus the number of carbon atoms of Al-C_n-Al structure. Here the symbols are the same as in Fig. 2. Inset shows the corresponding DOS.

$$E_{11} = -T_1\rho_1 + 1/4. \tag{12}$$

Since the oscillation amplitude of ρ_1 is much smaller than that of T_1, we conclude that the oscillation of E_{11} or G_I at low frequencies is mainly determined by the oscillation of dc conductance whose mechanism has been explained in detail by Lang.[4]

In order to further analyze the dynamic conductance, we plot G_R-G_{dc} as a function of frequency for different n in Fig. 5, where G_{dc} is the dc conductance. Different from the linear variation of G_I, G_R-G_{dc} shows quadratic dependence on frequencies. This is reasonable because G_R-G_{dc} is proportional to ω^2 according to Eq. (5) when neglecting the $O(\omega^n)(n \geq 4)$ terms. Figure 5 shows that the increasing rate of G_R-G_{dc} for the even number of carbon atoms is a little larger than that for the odd number of carbon atoms. In low frequencies, the oscillation of G_R-G_{dc} against the even-odd number of carbon atoms corresponds to the oscillation of dynamic dissipation K_{12}. Since there is no general relation between transmission coefficient (or DOS) and K_{12}, it is difficult to understand the oscillation of K_{12} from behaviors of transmission coefficient or DOS. However, if the transmission coefficient assumes Breit-Wigner form, K_{12} can be expressed according to Eqs. (1) and (7) (Ref. 31):

$$K_{12} = \frac{\pi^2\Gamma}{3}\left(\frac{dN}{dE}\right)^3 - \frac{2\pi^3}{\Gamma}\left(\frac{dN}{dE}\right)^2, \tag{13}$$

where dN/dE is given by

$$\frac{dN}{dE} = \frac{1}{2\pi}\frac{\Gamma}{(\Delta E)^2 + (\Gamma/2)^2} \tag{14}$$

that is shown in the inset of Fig. 5. Since DOS has even-odd oscillation, it is understandable that K_{12} shows similar behavior.

Physically, the behaviors of G_I and G_R-$G_{\rm dc}$ at small frequency can be understood qualitatively from a classical circuit model.[32] Classically, the dynamic conductance can be described as a *R*-*L* circuit if the system shows inductivelike behavior,

$$G_{RL}(\omega) = \frac{1}{R} + i\frac{\omega L}{R^2} - \frac{\omega^2 L^2}{R^3}. \quad (15)$$

While if the system behaves capacitivelike the system can be modeled as a *R*-*C* circuit with the dynamic conductance,

$$G_{RC}(\omega) = -i\omega C + \omega^2 C^2 R. \quad (16)$$

For a *R*-*L* circuit, the real part of G_{RL} decrease when the frequency is switched on. In addition, a positive imaginary part means that the voltage follows the current. While for a *R*-*C* circuit, the real part of dynamic conductance increases as we increase frequency and a negative imaginary part indicates the fact that the current follows the voltage. Obviously, our result for Al-C_n-Al structures is consistent with the behavior of *R*-*C* circuit for both even and odd *n* at low frequencies.

In the above discussion, we see that the atomic wire in the scattering region plays a major role in the conductance oscillation. Hence our result for carbon wires should remain for other electrodes such as Au. We also expect that our result applies to other atomic wires in the scattering region such as Na, Cs, Cu, Ag, and Au where even-odd oscillation for dc conductance was observed.[33] However, we think our result may not apply to Al wire in the scattering region since for Al wire four-atom period oscillation was found.[34]

In summary, we have calculated the dynamic conductance of Al-C_n-Al structures using the first-principles NEGF+DFT method. We found that at low frequencies, the dynamic conductance (both real and imaginary parts) oscillates for even-odd number of carbon atoms. In addition, the frequency dependent part of the dynamic conductance $G(\omega)$-$G_{\rm dc}$ depends only on the parity of the number of carbon atoms. Although the systems of carbon chain are quite transmissive with total transmission coefficient larger than 1/2, the emittance E_{11} are all positive indicating capacitivelike behaviors. This is because when there are more than one transmission channels at the Fermi level as the case we studied here, it is the average transmission $T_{\rm av}$ that determines the response of the dynamic systems.

ACKNOWLEDGMENT

We gratefully acknowledge support by a RGC grant from the HKSAR under Grant No. HKU 704607P.

*jianwang@hkusub.hku.hk

[1] C. Joachim, J. K. Gimzewski, and A. Aviram, Nature (London) **408**, 541 (2000).
[2] A. Nitzan and M. A. Ratner, Science **300**, 1384 (2003).
[3] A. Yazdani, D. M. Eigler, and N. D. Lang, Science **272**, 1921 (1996).
[4] N. D. Lang, Phys. Rev. B **55**, 9364 (1997); N. D. Lang and Ph. Avouris, Phys. Rev. Lett. **84**, 358 (2000).
[5] C. C. Wan, J.-L. Mozos, G. Taraschi, J. Wang, and H. Guo, Appl. Phys. Lett. **71**, 419 (1997).
[6] J. L. Mozos, C. C. Wan, G. Taraschi, J. Wang, and H. Guo, Phys. Rev. B **56**, R4351 (1997).
[7] Y. D. Wei, Y. Xu, J. Wang, and H. Guo, Phys. Rev. B **70**, 193406 (2004).
[8] P. Gambardella *et al.*, Phys. Rev. Lett. **93**, 077203 (2004).
[9] B. Larade, J. Taylor, H. Mehrez, and H. Guo, Phys. Rev. B **64**, 075420 (2001).
[10] R. Pati, M. Mailman, L. Senapati, P. M. Ajayan, S. D. Mahanti, and S. K. Nayak, Phys. Rev. B **68**, 014412 (2003).
[11] H.-S. Sim, H.-W. Lee, and K. J. Chang, Phys. Rev. Lett. **87**, 096803 (2001).
[12] P. Major, V. M. Garcia-Suarez, S. Sirichantaropass, J. Cserti, C. J. Lambert, J. Ferrer, and G. Tichy, Phys. Rev. B **73**, 045421 (2006).
[13] N. D. Lang and Ph. Avouris, Phys. Rev. Lett. **81**, 3515 (1998).
[14] B. Wang, Y. X. Xing, L. H. Wan, Y. D. Wei, and J. Wang, Phys. Rev. B **71**, 233406 (2005); Carbon **43**, 2786 (2005).
[15] R. H. M. Smit, C. Untiedt, G. Rubio-Bollinger, R. C. Segers, and J. M. van Ruitenbeek, Phys. Rev. Lett. **91**, 076805 (2003).
[16] C. C. Wan, J.-L. Mozos, J. Wang, and H. Guo, Phys. Rev. B **55**, R13393 (1997).
[17] M. Büttiker, A. Prêtre, and H. Thomas, Phys. Rev. Lett. **70**, 4114 (1993).
[18] M. Büttiker and T. Christen, in *Mesoscopic Electron Transport*, edited by L. L. Sohn *et al.* (Kluwer, Dordrecht, 1997), p. 259.
[19] B. G. Wang, J. Wang, and H. Guo, Phys. Rev. Lett. **82**, 398 (1999).
[20] T. Christen and M. Buttiker, Phys. Rev. Lett. **77**, 143 (1996).
[21] J. L. Wu, B. G. Wang, J. Wang, and H. Guo, Phys. Rev. B **72**, 195324 (2005).
[22] D. Waldron, P. Haney, B. Larade, A. MacDonald, and H. Guo, Phys. Rev. Lett. **96**, 166804 (2006).
[23] D. Waldron, V. Timoshevskii, Y. Hu, K. Xia, and H. Guo, Phys. Rev. Lett. **97**, 226802 (2006).
[24] P. Ordejón, E. Artacho, and J. M. Soler, Phys. Rev. B **53**, R10441 (1996); J. M. Soler, E. Artacho, J. D. Gale, A. García, J. Junquera, P. Ordejón, and D. Sánchez-Portal, J. Phys.: Condens. Matter **14**, 2745 (2002).
[25] N. Troullier and J. L. Martins, Phys. Rev. B **43**, 1993 (1991).
[26] J. Taylor, H. Guo, and J. Wang, Phys. Rev. B **63**, 245407 (2001); **63** 121104 (2001).
[27] M. Büttiker and T. Christen, in *Quantum Transport in Semiconductor Submicron Structures*, edited by B. Kramer (Kluwer Academic Publishers, Dordrecht, 1996), p. 263.
[28] T. Gramespacher and M. Buttiker, Phys. Rev. B **56**, 13026 (1997).
[29] When frequency approaches to 10 THz, it may be difficult to check our results experimentally.

[30] In the discrete potential approximation (Ref. 20), ρ_n is the projection of DOS on ϕ_n. Going beyond this approximation, ρ_n has to be obtained through Eq. (10).
[31] W. Zheng, Y. D. Wei, J. Wang, and H. Guo, Phys. Rev. B **61**, 13121 (2000).
[32] A. Pretre, H. Thomas, and M. Büttiker, Phys. Rev. B **54**, 8130 (1996).
[33] H. S. Sim, H. W. Lee, and K. J. Chang, Phys. Rev. Lett. **87**, 096803 (2001); Y. J. Lee, M. Brandbyge, M. J. Puska, J. Taylor, K. Stokbro, and R. M. Nieminen, Phys. Rev. B **69**, 125409 (2004).
[34] K. S. Thygesen and K. W. Jacobsen, Phys. Rev. Lett. **91**, 146801 (2003).